ELSEVIER

Journal of Power Sources 96 (2001) 329–336

JOURNAL OF POWER SOURCES

www.elsevier.com/locate/jpowsour

Mixed-reactant, strip-cell direct methanol fuel cells

S. Calabrese Barton[a,*], T. Patterson[b], E. Wang[b], T.F. Fuller[b], A.C. West[c]

[a]*The University of Texas at Austin, Austin, TX 78712, USA*
[b]*International Fuel Cells, South Windsor, CT 06074, USA*
[c]*Columbia University, New York, NY 10027, USA*

Received 23 October 2000; accepted 7 November 2000

Abstract

A feasibility analysis of a mixed-reactant, strip-cell direct methanol fuel cell concept is presented. In this type of cell, selective electrodes are mounted in an alternating fashion on the same side of a membrane electrolyte, and are exposed to a mixed-reactant feed. The presence of a single feed stream reduces flow system volume and sealing requirements, and potentially increases power density. Experimental polarization measurements of selective anodes and cathodes demonstrate the insensitivity of such electrodes to the presence of a mixed-reactant feed. The fuel efficiency of the direct methanol cell with selective electrodes is shown to be higher than that of a cell with more typical electrodes at low current density. The effect of geometric parameters on the performance of strip cells is discussed, and design recommendations are given for a simple geometry.

Keywords: Direct methanol fuel cells; Selective electrodes; Fuel efficiency; Methanol crossover

1. Introduction

High power density, small-scale direct methanol fuel cell stacks require minimization of weight and volume due to ancillary system components. One way to accomplish this is to use a ''strip-cell'' arrangement, in which strips of anode and cathode material are alternated over strips of membrane electrolyte on the same side of a non-conducting support film. A diagram of this scheme is shown in Fig. 1. This approach reduces weight and volume by reducing or eliminating seals, separator plates, and load-bearing structures.

Previous reports have considered the merits of conventional strip cells, in which the cells are arranged in-plane, but the reactants are separated on opposite sides of the cell [1–3]. Such designs provide high stack voltage in a small volume, but require complicated sealing to prevent leaks between reactant streams.

An alternative design approach is to use selective electrodes that are active only to one reactant. Using such electrodes, the feed streams can be mixed, and sealing issues become less important. Selective electrode fuel cells with mixed-reactant feed have been considered for solid oxide [4] and proton-exchange membrane fuel cells [5,6]. Dyer, in particular, achieved an enigmatic selectivity using noble-metal electrodes and a thin-film polymer electrolyte [1].

For the direct methanol cathode, selectivity is accomplished by using oxygen reduction catalysts that do not oxidize methanol. Two catalysts of current interest are iron tetramethoxyphenyl porphyrin (FeTMPP), and a transition metal cluster catalyst (Ru-Se-Mo). Both catalysts have been shown to be methanol tolerant [7,8]. Anodic selectivity is typically achieved by impregnating the electrode with hydrophilic materials; polytetrafluorosulfonic acid (PFSA), for example, excludes gases when flooded with water. Steady-state polarization performance of such electrodes will be presented.

The main motivation for development of these selective cathode catalysts has been to reduce the effect of methanol crossover. With 1 M methanol and Nafion® 117 PFSA membrane, the equivalent of about 200 mA/cm^2 of methanol diffuses across the membrane and combusts on the cathode [9]. Consequently, the fuel efficiency of the system is reduced, and more importantly, at low current densities the efficiency approaches zero. As will be demonstrated, an important advantage of the selective electrode approach for direct methanol fuel cells, including the strip-cell configuration, is that methanol crossover is eliminated as an issue.

The major drawback of using selective electrocatalysts has been their lower mass-specific catalytic activity

* Corresponding author. Fax: +1-512-471-8879.
E-mail address: scb@mail.utexas.edu (S.C. Barton).

0378-7753/01/$ – see front matter
PII: S0378-7753(00)00663-7

Nomenclature

i_{avg}	average cell current density (mA/cm^2)
I	cell current (mA)
L	electrode length (cm)
N_a	rate of methanol consumption at the anode (mol/s)
N_{XO}	methanol crossover rate (mol/s)
P	cell power density, defined by Eq. (2) (W/cm^2)
R	cell resistance (Ω)
s	electrode spacing (cm)
t	membrane thickness (cm)
V	cell potential (V)
V_Ω	cell potential drop due to Ohmic resistance (V)
w	anode and cathode width (cm)
w_a	anode width (cm)
w_c	cathode width (cm)
Greek letters	
ΔH	heat of combustion of methanol (J/mol)
Γ	dimensionless cell resistance ($L\kappa R$)
κ	electrolyte conductivity (mS/cm)

compared to noble metals such as platinum. Selective electrode kinetics may be improved by increased electrocatalytic activity, or by increasing catalyst mass loading or utilization. Nonetheless, such kinetic limitations must be overcome in order to make selective electrocatalysts feasible.

Even in the presence of strong kinetic limitations, the strip-cell geometry places a premium on electrolyte and electrode conductivity, because current flows perpendicular to the thickness of these components. Proper electrolyte-membrane thickness, electrode widths, and electrode spacing must be chosen to minimize Ohmic losses and maximize electrode utilization. This paper will conclude with a discussion of these issues.

2. Experimental

In the following measurements, a test cell of 32 cm^2 area was used, at a cell temperature of 80°C and ambient pressure. For selective-anode testing, a membrane-electrode assembly (MEA) with a Pt-Ru black (5 mg/cm^2) anode, Pt-black (5 mg/cm^2) cathode and Nafion® 117 electrolyte was fabricated. Aqueous methanol (1 M) was fed to the anode at a rate of 3 cm^3/min. Hydrogen was evolved on the cathode, which also served as a reference electrode. For mixed-reactant testing, 1 dm^3/min of either dry nitrogen or air was fed to the anode with the methanol.

For the cathode, MEAs were prepared using either FeTMPP or Ru-Se-Mo at 5 mg/cm^2 loading. Teflon was added to enhance hydrophobicity. The cathode was supplied with 3 dm^3/min of air. For mixed-reactant testing, 3 cm^3/min of methanol (1 M) was added to the air. Hydrogen was oxidized on the anode, which also served as the reference electrode.

An identical cell with both the selective Pt-Ru anode and the FeTMPP selective cathode was fabricated and tested in the conventional, bipolar configuration. For normal flow conditions, the anode was supplied with 3 cm^3/min of methanol (1 M) and the cathode was supplied with 3 dm^3/min of air. For mixed-reactant testing, the anode and cathode were both supplied with 3 cm^3/min of methanol (1 M) and 3 dm^3/min air. A cell with both the selective anode and Ru-Se-Mo cathode catalyst has not been tested. However, the performance of such a cell was estimated from the separate anode and cathode polarization tests.

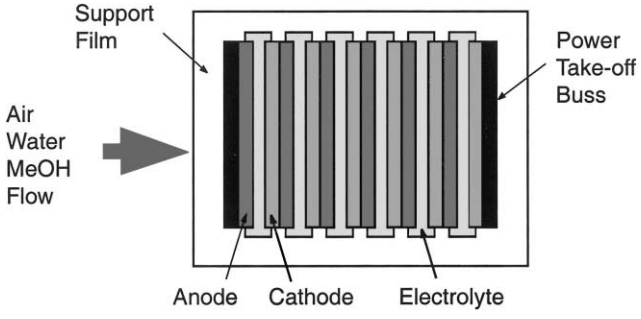

Fig. 1. Strip-cell concept.

3. Results

3.1. Selective anode polarization

A polarization curve for the selective anode is shown in Fig. 2. Data are given for polarization with 1.0 M methanol feed alone, and for mixed feeds with either nitrogen or air

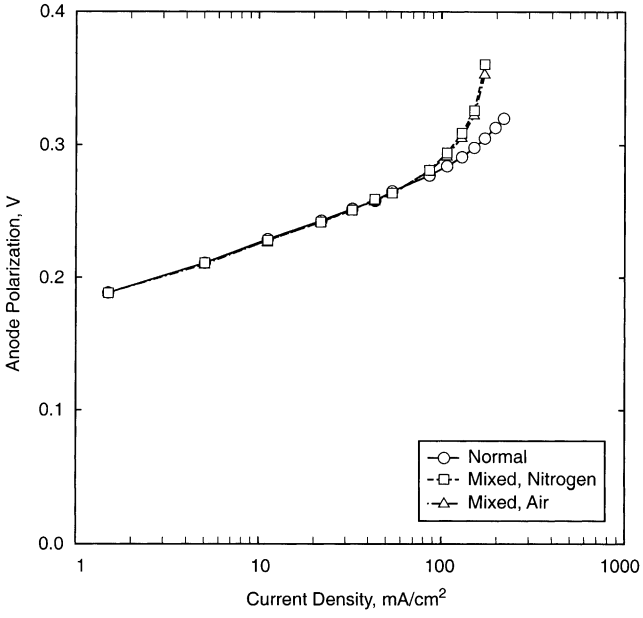

Fig. 2. Effect of mixed methanol-air feed on anode polarization.

added. All three curves are identical for current densities less than 100 mA/cm^2, where Tafel-like polarization prevails. Beyond this point, positive deviations from Tafel polarization appear. Both mixed-feed curves show similar, strong deviation, whereas the deviation is weaker for the solution alone. The addition of nitrogen therefore has the same effect in the high current density range as addition of air. Such a result suggests that the largest effect of the added gas was to impede mass transfer of methanol to the anode surface. Added oxygen therefore does not lead to parasitic methanol oxidation at the anode. To corroborate these findings, the anode-exit carbon dioxide levels were also measured. These levels agreed with predicted values calculated from cell current.

3.2. Selective cathode polarization

Polarization curves for two selective cathodes are given in Fig. 3. For the FeTMPP catalyst, the addition of methanol to the cathode feed results in a potential loss of about 40 mV. For the Ru-Se-Mo catalyst, the addition of methanol results in a small potential increase at low current densities, and a potential decrease at high current density. For the latter catalyst, one may conclude that the mixed-feed stream had no net effect on cathode polarization.

The cathode-exit carbon dioxide concentration was not detectable for either catalyst. As was found for the anode, therefore, the observed effects of mixed-reactant flow are attributable to mass transfer.

3.3. Complete cell polarization

Polarization measurements of a complete, selective-electrode, bipolar cell are given in Fig. 4. The cathode catalyst for the measured data was FeTMPP. The given data for the Ru-Se-Mo catalyst were estimated from the individual electrode measurements.

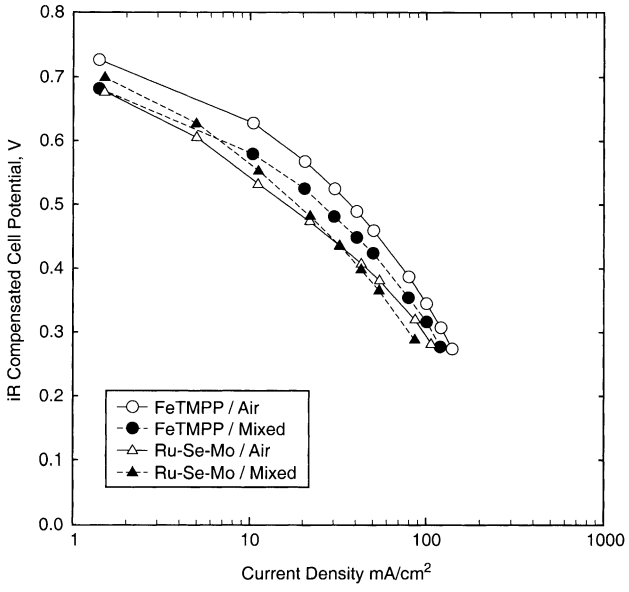

Fig. 3. Effect of mixed methanol-air feed on cathode polarization.

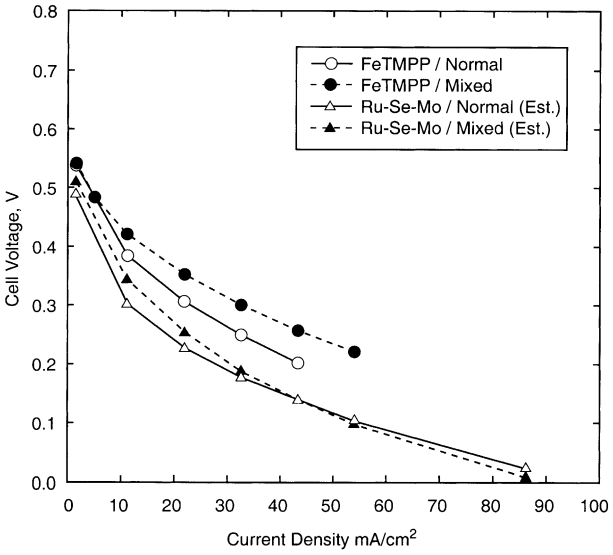

Fig. 4. Complete cell polarization performance.

The full-cell polarization data show no deleterious effect of mixed-reactant feed at the current densities considered. Such a result is expected because the mixed-reactant feeds primarily affected mass transfer for the individual anode and cathode measurements, and in the present range of current density, one would expect minimal mass transfer effects. The measured data for the FeTMPP cathode catalyst in fact show an increase in cell potential at finite current density. Although this result has not been completely explained, it indicates that polarization losses using the selective-catalyst electrodes are not substantial.

3.4. Fuel efficiency

As previously stated, an important advantage of selective electrodes for direct methanol fuel cells is the elimination of the issue of methanol crossover. This can be demonstrated in Fig. 5. Here the performance and the fuel efficiency of a selective-electrode cell with FeTMPP cathode catalyst and mixed feeds are compared with a more "traditional" DMFC with platinum catalysts and pure feeds. For these cells a constant rate of methanol crossover, $N_{XO} = 0.35$ mmol/cm^2/s, was assumed, equivalent to a crossover current density of 200 mA/cm^2. The fuel efficiency is defined by

$$\eta = \frac{IV}{\Delta H(N_a + N_{XO})} \quad (1)$$

where ΔH is the heat of combustion of the fuel, for which pure methanol at 20°C and 1 atm is 0.78 MJ/mol.

Although the performance of the "traditional" cell is better, its fuel efficiency is lowest at low current density. The cell with mixed-reactants and selective electrodes has an efficiency that is proportional to the cell potential. This

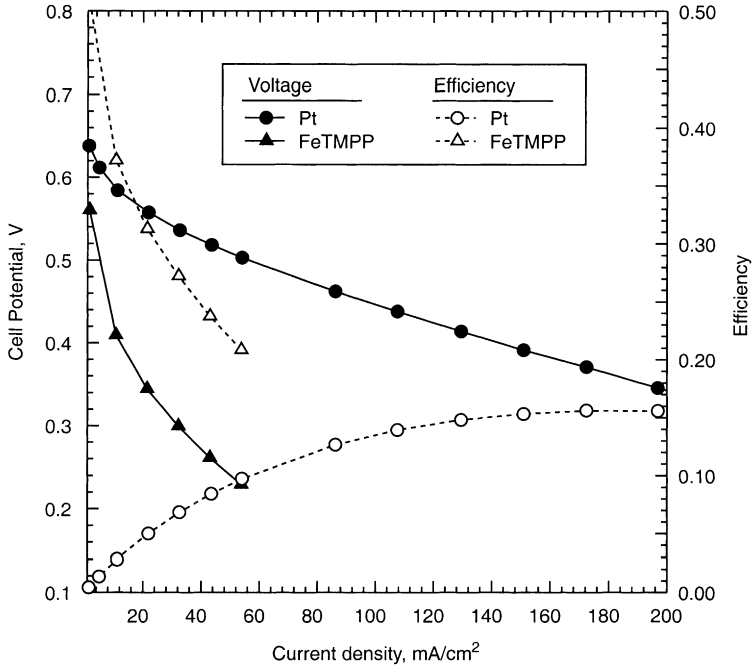

Fig. 5. Polarization and fuel efficiency of a traditional DMFC compared to one with selective electrodes. The efficiency of the selective-electrode cell is highest at low current density, whereas that of traditional cell increases with current density.

highlights the key advantage of the selective electrodes. High fuel efficiency can be achieved if the selective-electrode cell is limited to low current density.

4. Design studies

The results presented above demonstrate the performance of selective electrodes in a mixed-reactant direct methanol fuel cell, and indicate that high fuel efficiency may be possible at low current density. However, implementation of such electrodes in a strip-cell configuration presents an additional challenge. As shown in Fig. 6a, current passes in the plane of a strip cell, normal to the thickness and along the width of the electrodes and the membrane electrolyte. Such conditions make the strip-cell prone to large Ohmic losses. An appropriate strip-cell geometry must be chosen to minimize such losses compared to those associated with electrode kinetics. In the following, the appropriate cell geometry will be discussed for a simple configuration.

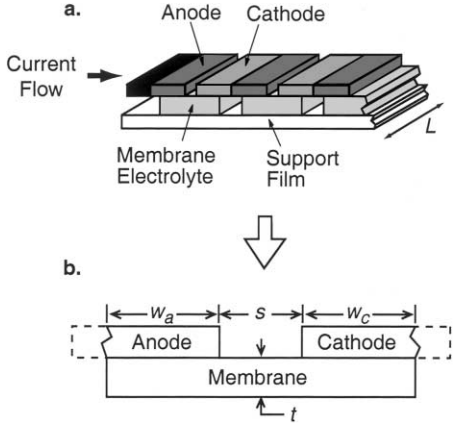

Fig. 6. Simplified strip-cell model.

4.1. Cell conditions

The strip-cell assembly of Fig. 6a was simplified to a two-dimensional model, as shown in Fig. 6b. The important parameters in this geometry are the electrode widths, w_c and w_a, the electrode spacing, s, and the thickness, t, of the membrane electrolyte. It is assumed here that the length, L, of the electrodes is much greater than their width or thickness. The width of each electrode is defined by the amount of overlap between the electrode and membrane. Base-case values for these parameters are specified in Table 1. For simplicity, a constant cell current density of 20 mA/cm^2 was assumed, although other design constraints may alternatively be chosen.

Table 1
Base-case cell parameters

Parameter	Value
Conductivity, κ (mS/cm)	100
Anode width, w_a (cm)	2×10^{-2}
Relative cathode width, w_c/w_a	1
Relative electrode spacing, s/w_a	0.1
Relative membrane thickness, t/w_a	2
Cell current density, i_{avg} (mA/cm^2)	20

Table 2
Kinetic parameters for selective electrodes

Parameter	Anode	FeTMPP cathode	Ru-Se-Mo cathode
Open circuit half-cell potential (V)	0.0	1.23	1.23
Exchange current density (mA/cm^2)	6.88×10^{-4}	4.95×10^{-6}	4.75×10^{-4}
Tafel slope (V)	2.25×10^{-2}	3.74×10^{-2}	6.58×10^{-2}

Each electrode is considered planar and infinitely conductive. Although electrode porosity is necessary for gas access, it was not considered here. High electrode conductivity may be practically achieved by addition of conductive filler such as graphite. Tafel kinetics were assumed; Tafel parameters, which are representative of the anode and two cathode materials discussed above, are given in Table 2. The assumption of Tafel kinetics is limited to current densities less than 100 mA/cm^2, such that mass-transfer effects may be neglected. The methods used for estimating cell performance are included in Appendix A.

4.2. Ohmic cell resistance

The Ohmic resistance, i.e. the cell resistance for infinitely fast electrode kinetics, provides a preliminary understanding of the effects of geometry on true cell resistance. Such information indicates the ranges of geometric parameters for which Ohmic losses may be minimized in the actual cell. Fig. 7 shows the variation of the dimensionless Ohmic resistance of the cell, $\Gamma = L\kappa R$, with electrode spacing, s, plotted with membrane thickness, t, as a parameter. In this plot, spacing and thickness are normalized by electrode width, w. As expected, the Ohmic resistance decreases uniformly with decreasing electrode spacing. In contrast, as thickness decreases, the Ohmic resistance is seen to increase. For $t/w > 2$ at small spacing, the resistance becomes essentially independent of thickness. For $s/w \leq 0.1$, this independence may be extended to $t/w = 1$. One may thus conclude that a practical design target is to set the electrode width to less than half the membrane thickness.

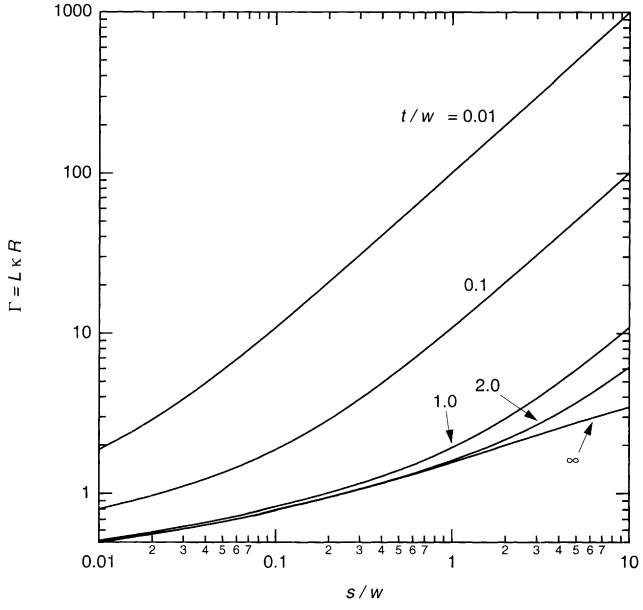

Fig. 7. Dimensionless resistance of strip cell, as calculated by Schwarz–Christoffel transformation. Resistance increases with increasing electrode spacing and with decreasing membrane thickness, and is independent of membrane thickness at high thickness and low spacing.

4.3. Overall cell polarization: effect of electrode width

The kinetics of the chosen selective cathode materials, as given in Table 2, are slow compared to supported noble metals. Such slow kinetics control the polarization behavior of the cell in cases where Ohmic losses are low, such as when the membrane thickness is large and the electrode spacing is small.

For example, Fig. 8 is a plot of cell power density as a function of electrode width, $w = w_a = w_c$, for two cathode materials. The values of all fixed parameters are given in Table 1. The power density is defined as

$$P = \frac{IV}{L(w_a + w_c + s)} \tag{2}$$

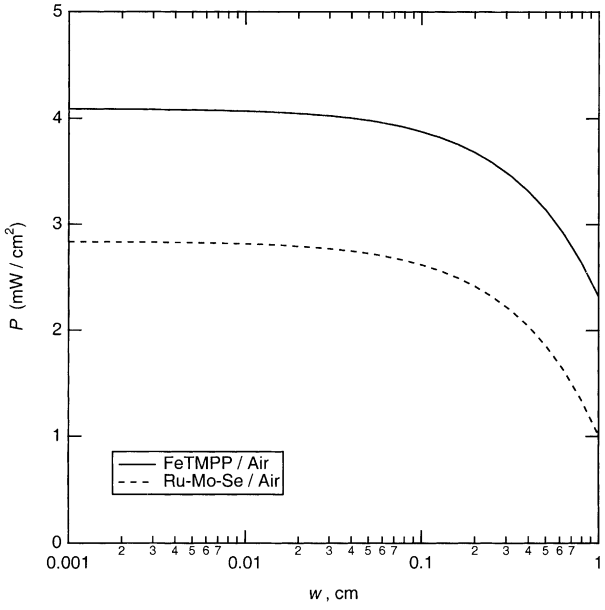

Fig. 8. Effect of electrode width on cell performance. Both cells are sensitive to electrode width for $w > 0.1$ cm.

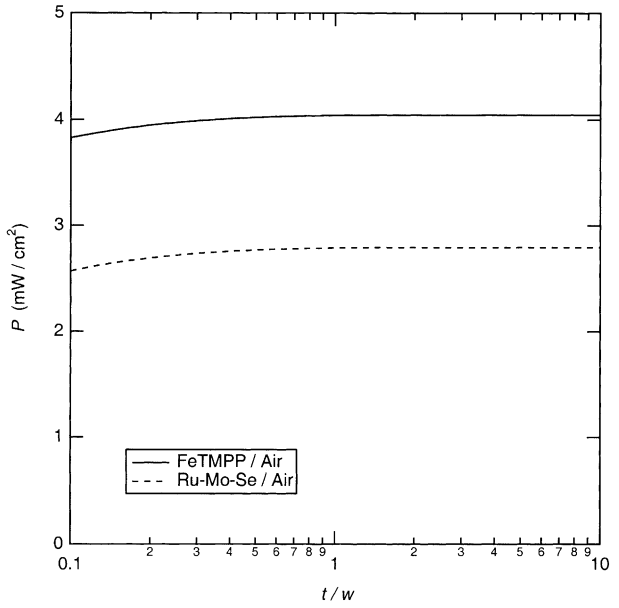

Fig. 9. Effect of membrane thickness on cell performance. The performance of both cells is weakly dependent on membrane thickness, and is independent of thickness for $t/w > 1$.

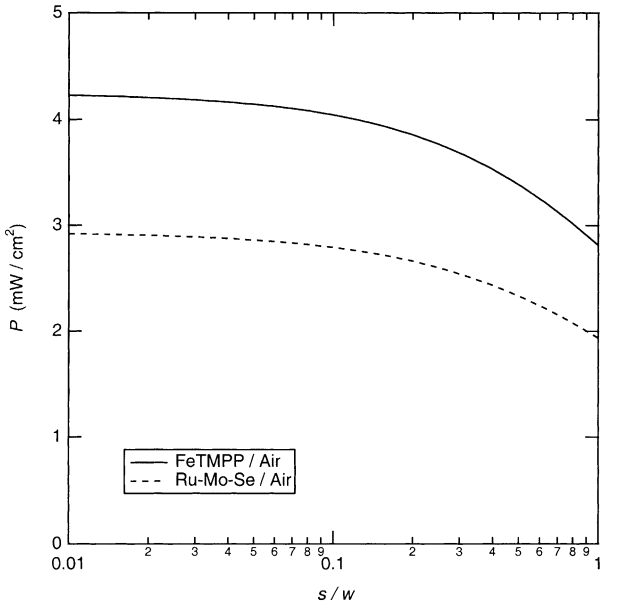

Fig. 10. Effect of electrode spacing on cell performance. Thickness dependence becomes weak for $s/w < 0.1$.

where the quantity $(w_a + w_c + s)$ is an estimate of total cell width. For both cathode materials, cell power density increases as electrode width decreases and Ohmic losses are reduced. The sensitivity of the power density to electrode width decreases with decreasing electrode width, however, as the cell polarization falls under the control of electrode kinetics. For both cell types, the power density begins to plateau as the electrode width decreases below 0.1 cm, and is insensitive to electrode width for $w < 0.01$ cm. For these electrode materials, therefore, an electrode size on the order of 0.1 cm may be appropriate.

4.4. Effect of membrane thickness

Fig. 9 shows the variation of cell power density with membrane thickness, with all fixed-parameter values given in Table 1. Power density appears to be only weakly dependent on membrane thickness over the range shown. As indicated by the primary cell resistance, the cell power density is independent of membrane thickness for $t/w > 1$. A relative membrane thickness of $t/w = 1.0$ is sufficient to minimize Ohmic losses under these conditions.

4.5. Effect of electrode spacing

In Fig. 10, the cell power density for a fixed cell current density is plotted as a function of electrode spacing for two cathode materials. Cell power density is shown to be only weakly dependent on electrode spacing for small spacing, such that $s/w < 0.1$. Under such conditions, cell polarization falls under mainly kinetic control. Under purely kinetic control, the electrode current density is uniform, and the electrode width, w, becomes an important length scale for current flow. As electrode spacing decreases to much less than this width, the potential drop across this width becomes small compared to the total Ohmic potential drop. One may conclude from these results that a normalized electrode spacing of $s/w = 0.1$ is the minimum from which practical benefit may be derived in this case.

4.6. Effect of relative electrode width

In a strip cell, electrodes of unequal macroscopic area can be employed in the same cell. Whether this added dimension can be exploited for performance gains depends on cell design criteria, e.g. whether cell potential or cell current is held fixed.

For example, Fig. 11 is a plot of cell power density as a function of cathode-anode width ratio, w_c/w_a, for two cathode materials. The values of all fixed parameters are given in Table 1, with the exception that cell potential, not current density, is held fixed at 0.4 V. For fixed potential, a weak maximum appears for electrode width ratio $w_c/w_a > 1$. For the Ru-Mo-Se catalyst, a 13% increase in power density can be achieved by setting the cathode width to be about three times that of the anode. This maximum occurs at a width ratio such that decreased cathode losses, due to lower cathode current density, are matched by anode losses that increase with increasing anode current density. In this case, the value of w_c/w_a at maximum power density is greater than unity because the cathode kinetics are slower than are those of the anode. It should be noted that such performance gains may also be obtained by increasing the cathode catalyst loading.

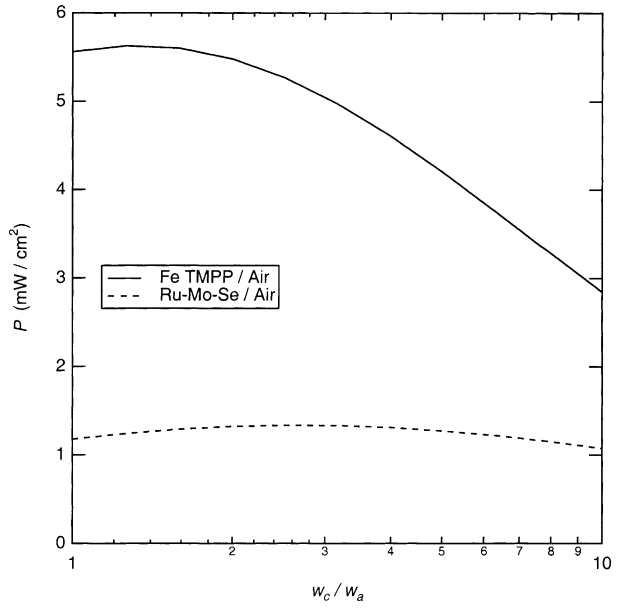

Fig. 11. Effect of cathode width on cell power density, at 0.4 V cell potential. The cell with Ru-Se-Mo cathode displays a strong maximum at $w_c/w_a = 3$. The maximum in the FeTMPP cell is weak.

No such maximum occurs for fixed cell current. Under electrode kinetic control, cell potential displays a weak, logarithmic dependence on cathode width; under resistance control, cell potential decreases with increasing cathode width. The linear increase in cell width therefore causes the fixed-current power density, as defined by Eq. (2), to decrease monotonically with increasing cathode width.

A strip cell with the FeTMPP cathode, in the base-case configuration, gives an Ohmic potential loss of only 4 mV at 20 mA/cm^2 current density. Such losses are small compared to the combined kinetic overpotential of about 800 mV. In terms of performance, therefore, the strip cell may be a practical configuration for the implementation of selective electrodes in a mixed-reactant, direct methanol fuel cell.

4.7. Effect of improved electrode kinetics

Improvements in the kinetic performance of both electrodes are likely, particularly with regard to the cathode. Such an advance would make higher cell current density more practical. In the limit of purely Ohmic resistance, cell polarization follows Ohm's law:

$$V_\Omega = \frac{\Gamma w}{\kappa} i_{\text{avg}} \tag{3}$$

where V_Ω is the cell potential drop due to Ohmic resistance, and i_{avg} is the average cell current density. Roughly speaking, therefore, increased current density would proportionally reduce the maximum practical electrode size such that a small value of V_Ω is maintained. The manufacturability of strip cells with such small electrode dimensions is a separate, important issue that will not be discussed here.

4.8. Overall system power density

The power densities presented herein should not be mistaken for overall system values; they only reflect the power density of the electrochemical cell itself. An estimate of overall system power density, the minimization of which is a main motivation for pursuit of mixed-reactant designs, requires detailed knowledge of a complete system, and will not be attempted here. Clearly, the power densities presented in Figs. 8–11 are quite low compared to conventional DMFC systems with noble metal catalysts. This is particularly true for the Ru-Se-Mo cathode, which gives only 1.2 mW/cm^2 at 20 mA/cm^2, compared to ~11 mW/cm^2 at the same current density for the platinum-cathode cell of Fig. 5. For the present strip-cell system to be practical, such deficiencies must be redressed by elimination of ancillary structures.

5. Conclusions

This paper has addressed important issues regarding the viability of a direct methanol fuel cell in a strip-cell configuration, with selective electrodes and a mixed-reactant feed. The polarization performance and selectivity of selective anode and cathode materials were demonstrated in a bipolar fuel cell with mixed-reactant feed. The effect of the mixed feed on the polarization was shown to be minimal. Deviations from Tafel-kinetic polarization were attributed to mass-transfer effects, and not parasitic oxidation of methanol. The performance of a combined selective-electrode fuel cell was also demonstrated to be insensitive to the presence of mixed-reactants. The fuel efficiency of the strip-cell configuration was shown to be higher than that of a bipolar cell with noble-metal electrodes at low current density.

A design analysis of a simple strip-cell DMFC withselective electrodes was conducted. For the electrode materials considered, the following geometry is appropriate.

1. An anode width of about 0.1 cm.
2. A membrane thickness 1 to 2 times the average electrode width.
3. An electrode spacing one tenth the average electrode width.

Additionally, the cathode width ratio may be chosen to be different from that of the anode to take advantage of mismatched electrode kinetics. For an electrode width of 0.02 cm, using FeTMPP cathode material, these dimensions lead to an Ohmic overpotential of just 4 mV at 20 mA/cm^2 cell current density. This demonstrates the viability of the strip-cell configuration for the mixed-reactant feed DMFC. A complete strip-cell is required to demonstrate that power-density improvements are achievable using such a configuration.

Acknowledgements

This work was supported by the Defense Sciences Office of DARPA under contract N00014-94-C-0290 through the Office of Naval Research.

Appendix A

The following is a description of the methods used to model the performance of the strip cell with geometry shown in Fig. 6.

A.1. Ohmic resistance

The dimensionless Ohmic resistance, $\Gamma = L\kappa R$, of the strip cell was calculated analytically by conformal mapping. The Schwarz–Christoffel method was used to map the 2D cell of Fig. 6a to a simple rectangular cell, the aspect ratio of which is equal to the dimensionless resistance of the original cell [10–13]. These calculations were performed using Mathematica, a computer software package for symbolic mathematics.

For this calculation, the anode and cathode were assumed to be of equal width, i.e. $w_c = w_a$, and electrode spacing and membrane thickness were scaled relative to electrode width. The dimensionless resistance was calculated for spacing and thickness, normalized by width, of 0.01–10.0.

A.2. Secondary current distribution

A boundary element method was used to simulate a single strip cell shown in Fig. 6b, using Tafel kinetic boundary conditions at both electrodes. These calculations were verified by comparing numerically obtained dimensionless resistance results to those obtained analytically, as described above. Under all conditions, numerical error was less than 5%.

References

[1] D. Modroukas, P. Rohonyi, O. Adlhart, in: Proceedings of the 37th Power Sources Conference, US Army Research Laboratory, Fort Monmouth, NJ, 1996, p. 85.
[2] R. Nolte, A. Kolbe, K. Ledjeff-Hey, in: Proceedings of the 37th Power Sources Conference, US Army Research Laboratory, Fort Monmouth, NJ, 1996, p. 77.
[3] A. Heinzel, R. Nolte, K. Ledjeff-Hey, M. Zedda, Electrochim. Acta 43 (1998) 3817.
[4] K. Asano, H. Iwahara, J. Electrochem. Soc. 144 (1997) 3125.
[5] G.A. Louis, J.M. Lee, D.L. Maricle, J.C. Trocciola, US Patent 4,248,941 (1981).
[6] C.K. Dyer, Nature 343 (1990) 547.
[7] S.Lj. Gojkovic', S. Gupta, R.F. Savinell, J. Electroanal. Chem. 462 (1999) 63.
[8] C. Fischer, N. Alonso-Vante, S. Fiechter, H. Tributsch, J. Appl. Electrochem. 25 (1995) 1004.
[9] F.J. Luczak, B.L. Murach, P.A. Plasse, D.L. Maricle, The Electrochemical Society Extended Abstracts, Vol. 96 (2), San Antonio, TX, 1996, p. 787 (Abstract).
[10] V.I. Ivanov, M.K. Trubetskov, Handbook of Conformal Mapping with Computer-Aided Visualization, CRC Press, Boca Raton, 1995, pp. 275–277.
[11] H.F. Moulton, Proc. London Math. Soc. 3 (2) (1905) 104.
[12] A.C. West, J. Newman, Determination of current distributions governed by Laplace's equation, in: B.E. Conway, J.O'M. Bockris, R.E. White (Eds.), Modern Aspects of Electrochemistry, No. 23, Plenum Press, New York, 1992, pp. 101–148.
[13] B.A. Fuchs, B.V. Shabat, Functions of a Complex Variable and Some of Their Applications, Vol. 1, Pergamon Press, New York, 1964, p. 394.